ASTRONOMY & ASTROPHYSICS
SUPPLEMENT SERIES

Astron. Astrophys. Suppl. Ser. **100,** 395-411 (1993)

Spectroscopic observations of radio source identifications from the 1 Jy, S4 and S5 Surveys. III.

M. Stickel and H. Kühr

Max-Planck-Institut für Astronomie; Königstuhl 17, D-W6900 Heidelberg 1, Germany

Received September 30; accepted December 3, 1992

Abstract. — Optical spectra are presented for the optical counterparts of 21 radio sources taken from the 1 Jy, S4, and S5 radio source catalogues. New redshifts are given for 18 sources, including a radio-selected quasar with a redshift of $z = 3.886$. For two other sources, redshifts had previously been listed in other publications and were confirmed by the new observations. Finally, one radio source is confirmed as a BL Lac object showing a featureless spectrum. For several sources, additional direct imaging data are provided.

Key words: galaxies: active — galaxies: distances and redshifts — quasars: emission lines — quasars: general — radio continuum: general

1. Introduction

Complete radio source catalogues are not only important for the study of the properties and evolutionary phenomena of the radio source population and their optical counterparts, they also provide the input for the investigation of the various unifying schemes of AGN and are potentially suitable to study the influence of small and large scale gravitational lensing on various source populations.

The 1 Jy (Kühr et al. 1981a), the S4 (Pauliny-Toth et al. 1978) and S5 (Kühr et al. 1981b, 1987) radio source catalogues, which are complete to consecutive flux limits of 1 Jy, 0.5 Jy, and 0.25 Jy at 5 GHz, respectively, have recently been utilized for a number of such studies. The 1 Jy catalogue has been used by Fugmann (1990) to search for associations between radio sources and bright galaxies, by Stickel et al. (1991, 1993b) for the investigation of a complete radio-selected sample of BL Lac objects, and by Padovani (1992a,b) and Padovani & Urry (1992) to test the unification of different classes of AGN. In addition, a number of 1 Jy sources are simultaneously monitored at radio and optical wavelength (Wagner et al. 1990). The S4 and S5 catalogues have been used for the selection of radio source samples which were subsequently studied with *VLBI* (Pearson & Readhead 1981, 1988; Witzel et al. 1988).

Those investigations show that there is considerable interest in these high frequency selected radio source catalogues, despite the fact that optical identifications and redshifts for the 1 Jy, S4, and S5 sources are as yet not complete. Spectroscopic data for 1 Jy and S5 catalogue sources have previously been given in Stickel et al. (1989) and Stickel et al. (1993a). As a further step to complete the optical identification status, this paper presents new optical spectra and redshifts for a number of 1 Jy, S4, and S5 radio sources. Additional CCD images supplement the spectroscopic data for those sources where the available direct imaging data is meagre or the identification status has been revised.

2. Observations and data reduction

The observed 1 Jy, S4, and S5 radio sources are listed in Table 1, 4, and 7, respectively. Each table lists for each object its name (Col. 1), other names (Col. 2), the radio position (Cols. 3, 4), the magnitude and the type of the optical counterpart (Cols. 5, 6), the 5 GHz flux (Col. 7), the radio spectral index between 11 and 6 cm (Col. 8), and finally, references to finding charts (Col. 9).

The spectroscopic data were obtained during four observing runs with the 2.2 m and 3.5 m telescopes on Calar Alto, Spain. Table 2, 5, and 8 give a journal of the observations of the 1 Jy, S4, and S5 sources, respectively. Each table lists for each observed object its name (Col. 1), the date of the observation (Col. 2), the telescope used (Col. 3), the integration time (Col. 4) and reciprocal dispersion of the final wavelength calibrated spectra (Col. 5).

For the observations with the 2.2 m telescope, a Boller & Chivens Cassegrain spectrograph was utilized. During the first run in November 1991 a 1150*790 GEC CCD (pixel size 22.5 μm) and during the second run in June 1992 a 1024*1024 Tektronix CCD (pixel size 24 μm) was used as a detector. For the observations at the 3.5 m telescope, we employed the Cassegrain Twin Spectrograph with a 1024*640 RCA CCD (pixel size 15 μm) with two-pixel on-chip binning along the wavelength direction in the blue and a 1150*790 GEC CCD (pixel size 22.5 μm) in the red channel. In each of the observing runs the spectra covered the wavelength range between $\approx$ 3500 Å and $\approx$ 9200 Å.

After debiasing and flatfielding, the one-dimensional spectra were extracted from the two-dimensional CCD data according to the algorithm of Horne (1986). In addition, the optimal extraction algorithm given by Robertson (1986) was used for the faint objects such as 2029+121, 2149+056, and 2255+416. Rebinning to a linear wavelength scale was carried out by fitting third order polynomials to HeAr comparison spectra, which were taken immediately before or after the object exposures. The one-dimensional spectra were flux calibrated by using observations of standard stars from the list of Massey et al. (1988) and Massey & Gronwall (1990), which had been treated in a similar way as the object spectra.

3. Results of the optical spectroscopy

The optical spectra of the observed 1 Jy, S4 and S5 radio sources are shown in Figs. 1, 2, and 3, respectively. The emission lines as well as the absorption lines of the stellar component of the galaxies have been identified, while intervening absorption line systems have been indicated with asterisks. In most spectra, atmospheric absorption features as well as residuals of strong night sky lines are present, but have not been marked.

Spectroscopic data for all except one (1926+611) of the 1 Jy, S4, and S5 sources are given in Table 3, 6, and 9, respectively. Each table lists for each object its name (Col. 1), its redshift (Col. 2), the observed absorption or emission features (Col. 3) along with their rest wavelengths (Col. 4), their observed wavelengths (Col. 5), and their individual redshifts (Col. 6), the FWHM (Col. 7), the observed equivalent width (Col. 8), and the emission line fluxes (Col. 9). Finally, Col. 10 contains some remarks. The wavelengths as well as the parameters of the emission and absorption lines have been derived from fits of one or (for broad lines with a narrow central component) two gaussians together with a linear continuum to the flux calibrated spectra.

To get the full wavelength coverage also with the Cassegrain spectrograph at the 2.2 m telescope, these observations were made without an order separation filter. Thus the first order spectra are contaminated at the red end ($\lambda \gtrsim 7000$ Å) by the second-order spectrum. This is usually not a problem, because most of the optical counterparts are red and/or have low fluxes in the blue, which will probably not introduce spurious features in the red part of the spectrum. The observed standard stars, however, were mainly hot white dwarfs in order to have sufficient signal in the blue. Thus, the spectra of the standard stars are definitely distorted for $\lambda \gtrsim 7000$ Å by the second order, which results in a spurious depression of the continuum of the calibrated object spectra. Two clear examples for this effect are the spectra of 0010+405 and 0836+710 (Fig. 1). While the derived redshifts are unaffected by this depression, the measured line fluxes and to some degree also the equivalent width of the broad emission lines are in error. Tables 3, 6, and 9 contain a note in Col. 10 for those emission lines, which are influenced by the uncorrected second order contamination, while the corresponding emission line data have been marked with a colon.

3.1. *Notes on individual 1 Jy sources*

0010+405: The optical counterpart has initially been identified by Kapahi (1979) with a $m = 17.9$ mag QSO. A direct CCD image, taken with the 3.5 m telescope on Calar Alto, Spain, in July 1990 (Fig. 4) confirms the optical brightness but shows that the optical counterpart is actually a galaxy without a strong central point source. The optical spectrum supports this classification since stellar absorption features of CaII, MgI and NaI at $z = 0.255$ are detected besides the [0 III] $\lambda\lambda$4959,5007 and Hα emission lines. The redshift of 0010+405 has previously been listed by Biermann et al. (1987), based on spectroscopic observations by one of us (H.K.) with the Steward Observatory 90″ telescope on Kitt Peak.

0836+710: The redshift of $z = 2.172$ is derived from two broad emission lines identified with CIV λ1549 and CIII] λ1909. The absorption feature at $\approx$ 5360 Å is identified with an intervening Mg II $\lambda\lambda$2796,2803 absorption line system at $z_{\rm abs} = 0.914$. A preliminary value for the redshift has previously been given by Eckart et al. (1986), which was based on spectroscopic observations by one of us (H.K.) with the Steward Observatory 90″ telescope on Kitt Peak.

2029+121: The direct image taken with the 3.5 m telescope on Calar Alto, Spain, in September 1989 (Fig. 4), shows a close pair of objects at the radio position, which was already noticed by Condon et al. (1977). The optical counterpart of 2029+121 is the fainter object to the west. Its brightness has been measured to be $m_R = 20.3$ mag, in contrast to the value of $m = 18.5$ mag listed by Condon et al. (1977), which may indicate optical variability.

The spectrum of 2029+121 shows only one readily visible feature, an absorption line doublet at $\lambda\lambda$ 5920,5934 Å which is identified with MgII $\lambda\lambda$2796,2803 at $z_{\rm abs} = 1.117$.

After this assignment has been made, a weak broad emission feature was noted just redward of the absorption lines, which has been associated with MgII λ2798 at $z = 1.223$. The corresponding redshifted CIII] λ1909 emission line may also be present at the expected wavelength. Because the emission features upon which the redshift is based are rather weak, the redshift is considered to be uncertain and further confirming observations are needed. Since the rest frame equivalent widths of the suspected emission lines are below the 5 Å limit used for the selection of BL Lac objects from the 1 Jy catalogue (Stickel et al. 1991, 1993b), 2029+121 is classified as a BL Lac object. Finally, it should be noted that the somewhat brighter object 2.5″ to the east is a K star.

2149+056: The optical counterpart of this radio source has been classified by Fugmann & Meisenheimer (1988) as a $m = 20.5$ mag probably extended QSO, while O'Dea et al. (1990) describe this object as a $m = 20.4$ mag galaxy with a central point source. A direct CCD image taken with 2.2 m telescope on Calar Alto, Spain, in June 1992, shows that 2149+056 is clearly extended along the northeast - southwest direction. The central point source may be variable since the galaxy component is more easily seen in Fig. 4 than in the direct image of O'Dea et al. (1990).

O'Dea et al. (1990) described the optical spectrum as featureless, characteristic for BL Lac objects. Our spectrum, however, shows emission lines of [O II] λ3727 and [Ne III] λ3869 as well as [0 III] $\lambda\lambda$4959,λ5007 at a redshift of $z = 0.740$. While [0 II], [Ne III] and [0 III] λ4959 are unresolved, the [0 III] λ5007 emission line is rather broad, possibly due to residuals of bright night sky lines. The classification as a BL Lac objected is rejected on the basis of the rest frame equivalent width of the emission lines, which are above the 5 Å limit used for the selection of BL Lac objects from the 1 Jy catalogue (Stickel et al. 1991, 1993b).

2255+416: This radio source has been identified by Rieke et al. (1979) with the northern component of a close pair of stellar objects (Fig. 4), for which the observations of Fugmann & Meisenheimer (1988) indicate optical variability. The optical spectrum of this counterpart shows a broad emission line at 6014 Å which may be indentified with Mg II λ2798 at $z = 1.149$. Another weak emission feature is possibly present near the expected position of the redshifted CIII]λ1909 emission line, but the agreement of the two individual redshifts is poor. Since the spectrum of the southern component shows the characteristic absorption throughs of a late type star, where one of the maxima of the spectrum falls close to the emission line at $\approx$ 6000 Å seen in 2255+416, we cannot exclude that this emission line is in fact caused by stray light from the southern star, added to a featureless power law continuum. Thus the redshift listed in Table 3 is regarded as uncertain, and confirming observations are needed. In any case the redshift listed by Bregman et al. (1985) could not be confirmed.

3.2. *Notes on individual S4 sources*

0344+405: For this radio source, two contradictory identifications have been given in the literature. Willson (1972) suggested as the optical counterpart a $m = 16.5$ mag galaxy lying between the two radio lobes. This identification has later been confirmed by Porcas et al. (1980). On the contrary, Bozyan (1979) classified the radio source as an optical blankfield.

The spectrum of the galaxy suggested by Willson (1972) as the identification shows rather weak absorption features of MgI λ5175 and NaI λ5893 as well as weak and narrow [NII] λ6584 emission at $z = 0.039$.

1152+51: Kapahi (1981) noted that this radio source is double, where the component B is associated with a $m = 16$ mag galaxy, the spectrum of which is shown in Fig. 2. The redshift of $z = 0.051$ has been derived from stellar absorption lines and a narrow emission line at 6918 Å, which has been identified with Hα λ6563, partially affected by the atmospheric B-band. We note, however, that the agreement of the individual redshifts is better, if the narrow emission line is identified with [N II] λ6584 at $z = 0.051$.

1452+502: This radio source has been identified by Machalski & Condon (1983) with an optical object of unspecified type. The magnitude of $m_R = 19.2$ mag and the classification as a QSO (Table 4) has been derived from a direct image taken with the 2.2 m telescope on Calar Alto, Spain, in June 1992 (Fig. 5). The spectrum of the QSO shows rather narrow Lyman α λ1216 and CIV λ1549 emission lines with FWHM corresponding to $\approx$ 1700 km s^{-1} and $\approx$ 2200 km s^{-1}, respectively, in the rest frame of the quasar. This object is thus a member of the small group of narrow line quasars (Baldwin et al. 1988). In addition, Lyman α has a broad component, which appears to be partially absorbed on the short wavelength side.

Since the original S4 catalogue (Pauliny-Toth et al. 1978) did not list a radio spectral index, the value given in Table 4 has been derived from the radio fluxes listed in Kühr et al. (1979).

1745+624: This radio source has initially been identified with a 19.5 mag galaxy (Kapahi 1979). A new direct CCD image taken with the 3.5 m telescope on Calar Alto, Spain, in June 1992, however, showed that the optical counterpart is actually a $m_R = 18.7$ mag unresolved quasar (Fig. 5), the redshift of which is $z = 3.886$ (Fig. 2). This value has been derived from the OVI λ1034, NV λ1240 and OI/SiI λ1306 emission features only, since Lyman α λ 1216 is self-absorbed on its blue wing while SiIV/OIV λ1402 and CIV λ1549 are affected by the atmospheric B-

and A-band, respectively. This object is one of the highest redshift quasars with strong radio emission. A more detailed description of the observations of this object is given in Stickel (1993). 1745+624 has been discovered independently as a high-redshift quasar by Becker et al. (1992).

1833+653: The optical spectrum is devoid of emission lines and the redshift of $z = 0.161$ is derived from stellar absorption lines.

1849+670: Emission lines of MgII λ2798, [0 III] λ3727, Hβ λ4861 and [0 III] $\lambda\lambda$4959,5007 at $z = 0.657$ are superposed on a power law continuum. A MgII $\lambda\lambda$2796,2803 absorption line doublet at $z_{\rm abs} = 0.533$ is detected on the blue side of MgII λ2798.

1926+611: The classification of 1926+611 as a BL Lac object (Kühr & Schmidt 1990) was based on spectroscopic observations by one of us (H.K.) with the Steward Observatory 90″ telescope on Kitt Peak, which showed a featureless spectrum. High optical polarization has subsequently been found by Kühr & Schmidt (1990). The new optical spectrum shown in Fig. 2 is also devoid of emission and absorption features, thereby confirming the BL Lac type nature of this object.

The radio spectral index given in Table 4 has been derived from the radio fluxes given in Kühr et al. (1979), since no value has been listed in the original S4 catalogue (Pauliny-Toth et al. 1978).

1943+546: The brightness of $m = 17.6$ mag for this galaxy has been derived from a direct image taken with the 3.5 m telescope on Calar Alto, Spain, in June 1992 (Fig. 5). The spectrum shows stellar absorption lines and narrow Hα at $z = 0.263$.

Cohen et al. (1977) noted that the galaxy identified with the radio source apparently lies at the center of a faint cluster. The direct image (Fig. 5), however, shows that four of the faint objects surrounding the galaxies are actually unresolved, and are thus probably stars, while only the object lying to the northeast is resolved; its morphology resembles that of a few other galaxies in the field.

3.3. *Notes on individual S5 sources*

1027+744: The optical spectrum shows a number of emission lines at $z = 0.123$, superposed on an underlying power law continuum. Although this object appears fuzzy on POSS (Kühr et al. 1987) and is thus classified as a galaxy, the absorption lines of the stellar component are rather weak and have not been marked in Fig. 3.

1042+736: Although this radio source is identified with the bright nearby galaxy NGC 3343 (de Ruiter et al. 1977; Kühr et al. 1987), no redshift has so far been available. The optical spectrum shows the characteristic absorption features of a late type galaxy at $z = 0.021$.

1616+851: The optical counterpart has previously been classified as a QSO lying about 4″ north of a galaxy (Kühr et al. 1987). A direct image taken in June 1992 with the 2.2 m telescope on Calar Alto, Spain, however, showed that the northern object has a resolved appearance and is thus a galaxy with $m_{\rm R} = 17.4$ mag, while the southern object is stellar (Fig. 6). The spectrum of the galaxy shows strong emission lines at $z = 0.183$. Hα λ6563 is affected by the atmospheric A-band and has not been used for the redshift determination. The unresolved object south of 1616+851 is found to be a late type star.

1733+737: The redshift of this galaxy is derived from stellar absorption features as well as [0 II] λ3727 and Hα/[NII] $\lambda\lambda$6563,6584 emission lines.

1807+707: The optical spectrum of this galaxy shows absorption lines of the stellar component at $z = 0.203$. Possibly, the single narrow emission line, which has been identified with Hα λ6563, may also be [N II] λ 6584.

1945+725: The optical counterpart of this radio source shows a rich emission line spectrum at $z = 0.303$. The Hα emission line has been fitted with two gaussians corresponding to the narrow and broad component (Table 9). The asymmetric red wing of the Hα line is likely to be an artifact of the flux calibration.

1946+708: The optical spectrum reveals low excitation emission lines of [0 II] λ3727, [0 I] λ6300, Hα/[N II]$\lambda\lambda$6563,6584 and [S II] $\lambda\lambda$6717,6737 as well as stellar absorption features at $z = 0.101$.

2111+801: A number of emission lines at $z = 0.524$ are detected in the optical spectrum of 2111+801. Hβ λ4861 shows a broad and a narrow component and has been fitted with two gaussians. [O III] λ5007 falls into the atmospheric A-band, which affects the line ratio of [O III] $\lambda\lambda$4959,5007 as well as the measured line flux.

References

Baldwin J.A., McMahon R., Hazard C., Williams R.E. 1988, ApJ 327, 103
Becker R.H., Helfand D.J., White R.L. 1992, AJ 104, 531
Biermann P.L., Kühr H., Snyder W.A., Zensus J.A. 1987, A&A 185, 9
Bregman J.N., Glassgold A.E., Huggins P.J., Kinney A.L., 1985, ApJ 291, 505
Bozyan E.P. 1979, AJ 84, 910
Cohen A.M., Porcas R.W., Browne I.W.A., Daintree E.J., Walsh D. 1977, MemRAS 84, 1
Condon J.J., Hicks P.D., Jauncey D.L. 1977, AJ 82, 692
de Ruiter H.R., Willis A.G., Arp H.C. 1977, A&AS 28, 211

Eckart A., Witzel A., Biermann P., Johnston K.J., Simon R., Schalinski C., Kühr H., 1986, A&A 168, 17
Fugmann W. 1990, A&A 240, 11
Fugmann W., Meisenheimer K. 1988, A&AS 76, 145
Horne K. 1986, PASP 98, 609
Kapahi V.K. 1979, A&A 74, L11
Kapahi V.K. 1981, A&AS 43, 381
Kühr H. 1977, A&AS 29, 139
Kühr H., Nauber U., Pauliny-Toth I.I.K., Witzel A. 1979, MPIfR Preprint No. 55
Kühr H., Witzel A., Pauliny-Toth I.I.K., Nauber U. 1981a, A&AS 45, 367
Kühr H., Pauliny-Toth I.I.K., Witzel A., Schmidt J. 1981b, AJ 86, 854
Kühr H., Schmidt G. 1990, AJ 99, 1
Kühr H., Johnston K.J., Odenwald S., Adlhoch J. 1987, A&AS 71, 493
Machalski J., Condon J.J. 1983, AJ 88, 143
Massey P., Strobel K., Barnes J.V., Anderson E. 1988, ApJ 328, 315
Massey P., Gronwall C. 1990, ApJ 358, 344
O'Dea C.P., Baum S.A., Morris G.B. 1990, A&AS 82, 261
Padovani P. 1992a, A&A 256, 399
Padovani P. 1992b, MNRAS 257, 404.
Padovani P., Urry C.M. 1992, ApJ 387, 449
Paulini-Toth I.I.K., Witzel A., Preuss E., Kühr H., Kellermann K.I., Fomalont E.B., Davis M.M. 1978, AJ 83, 451
Pearson T.J., Readhead A.C.S. 1981, ApJ 248, 61
Pearson T.J., Readhead A.C.S. 1988, ApJ 328, 114
Porcas R.W., Urry C.M., Browne I.W.A., Cohen A.M., Daintree E.J., Walsh D. 1980, MNRAS 191, 607
Rieke G.H., Lebofsky M.J., Kinman T.D. 1979, ApJL 232, L151
Robertson J.G. 1986, PASP 98, 1220
Shimmins A.J., Bolton J.G., Wall J.V. 1975, AJPAS N34, 63
Stickel M., Fried J.W., Kühr H. 1989, A&AS 80, 103
Stickel M., Padovani P., Urry C.M., Fried J.W., Kühr H. 1991, ApJ 374, 431
Stickel M., Kühr H., Fried J.W. 1993a, A&AS 97, 483
Stickel M., Fried J.W., Kühr H. 1993b, A&AS 98, 393
Stickel M. 1993, A&A, in press
Stickel M. 1992, A&A, submitted
Wagner S., Sanchez-Pons F., Quirrenbach A., Witzel A. 1990, A&A 235, L1
Wills D. 1967, MNRAS 135, 339
Willson M.A.G. 1972, MNRAS 156, 7
Witzel A., Schalinski C.J., Johnston K.J., Biermann P.L., Krichbaum T.P., Hummel C.A., Eckart A. 1988, A&A 206, 245

Table 1. Observed 1 Jy radio sources

Object	other Name	RA (1950)	Dec (1950)	m	type	S_{5GHz}	α_{11-6}	FC
(1)	(2)	(3)	(4)	(5)	(6)	(7)	(8)	(9)
0010+405	4C+40.01, S4 DA 06	00 10 54.26	+40 34 57.0	17.9	Gal[a]	1.05	-0.23	0,1
0836+710	4C+71.07, S5	08 36 21.63	+71 04 21.9	16.5	QSO	2.59	-0.32	2
2029+121	MG 2031+1219, PKS OW+149	20 29 32.68	+12 09 28.8	20.3[b]	QSO/BL	1.33	+0.74	0,3
2149+056	MG 2151+0552, PKS OX+082	21 49 07.66	+05 38 07.4	20.4	Gal	1.04	+0.05	0,4
2255+416	4C+41.45, DA 589, S4 OY+492	22 55 04.66	+41 38 13.2	20.9	QSO	1.00	-0.55	0,5

References : 0.) this paper 1.) Kapahi (1979) 2.) Kühr et al. (1987)
3.) Shimmins (1975) 4.) O'Dea et al. (1990) 5.) Rieke et al. (1979)

a) revised classification, see notes on individual objects

b) revised magnitude and classification, see notes on individual objects

Table 2. Journal of the observations of 1 Jy identifications

Object	date	telescope [a]	int.time [sec]	scale [Å/pixel]
(1)	(2)	(3)	(4)	(5)
0010+405	Nov 23/26, 1991	CA 2.2	8000	4.9
0836+710	Nov 24, 1991	CA 2.2	3600	4.9
2029+121	July 29, 1990	CA 3.5	4000	4.3/3.6 [b]
2149+056	July 2/3 1992	CA 3.5	8000	4.3/3.6 [b]
2255+416	July 29, 1990	CA 3.5	4000	4.3/3.6 [b]

[a] CA 3.5 and CA 2.2 denote the 3.5m and the 2.2m telescopes on Calar Alto, Spain.

[b] Twin spectrograph blue and red channel dispersion, respectively.

Table 3. Emission and absorption line data for 1 Jy sources

Object	<z>	ID	λ_0 [Å]	λ_{obs} [Å]	z_{ind}	FWHM [Å]	EW_{obs} [Å]	Flux [10^{-16} erg/s/cm^2]	Remarks *
(1)	(2)	(3)	(4)	(5)	(6)	(7)	(8)	(9)	(10)
0010+405	0.255	CaII	3933	4935	0.255				gal
		CaII	3968	4973	0.253				gal
		OIII	4959	6227	0.256	14.3	3.1	2.3:	cal
		OIII	5007	6289	0.256	10.3	6.1	4.4:	cal
		MgI	5175	6499	0.256				gal
		NaI	5893	7398	0.255				gal
		Hα	6563	8249	0.257	66.3	29.0:	14.9:	cal
0836+710	2.172	CIV	1549	4924	2.179	96.3	33.5	103.9	
		CIII	1909	6041	2.164	242.4	63.6:	175.3:	cal
		MgII	2796	5352	0.914				abs
		MgII	2803	5367	0.915				abs
2029+121	1.215	CIII	1909	4213	1.207	64.0	9.2	5.1	
		MgII	2798	6220	1.223	104.8	10.8	5.6	
		MgII	2796	5916	1.117				abs
		MgII	2803	5934	1.117				abs
2149+056	0.740	OII	3727	6486	0.740	21.7	21.2	1.7	
		NeIII	3869	6733	0.740	19.0	8.1	0.8	
		OIII	4959	8622	0.739	18.9	14.5	2.6	
		OIII	5007	8689	0.735	52.1	86.2	13.2	
2255+416	1.121	CIII	1909	3996	1.149	93.9	691.1	9.2	
		MgII	2798	6014	1.093	113.6	83.9	9.4	

*Abbreviations :
- abs : intervening absorption lines
- cal : equivalent width and emission line flux uncertain due to uncorrected second order contamination of standard star spectra
- gal : stellar absorption lines of host galaxy

Table 4. Observed S4 radio sources

Object	other Name	RA (1950)	Dec (1950)	m	type	S_{5GHz}	α_{11-6}	FC
(1)	(2)	(3)	(4)	(5)	(6)	(7)	(8)	(9)
0344+405	4C+40.12, OE+475	03 44 38.70	+40 34 39.0	16.5	Gal	0.502	-0.57	3
1152+551	4C+55.22, OM+588 VV 9.20.31, DA 314	11 52 52.00	+55 10 16.0	16.0	Gal	0.843	-0.73	1
1452+502	3C 308, 4C+50.40 OQ+587	14 52 29.49	+50 15 39.5	19.2	QSO[b]	0.540	-0.78	0,2
1745+624	4C+62.29, OT+676	17 45 48.10	+62 27 52.0	18.7	QSO[a]	0.578	+0.02	0,4
1833+653	3C 383, 4C+65.23 DA 458	18 33 33.70	+65 19 11.0	17.0	Gal	0.799	-0.70	5
1849+670	4C66.20	18 49 16.50	+67 02 07.9	18.0	QSO	0.590	-0.76	6
1926+611		19 26 49.65	+61 11 21.1	17.5	QSO/BL	0.721	-0.09	1
1943+546	OV+573	19 43 22.70	+54 40 48.0	17.7	Gal	0.850	-0.55	0,7

References : 0.) this paper 1.) Kapahi (1981) 2.) Machalski & Condon (1983)
3.) Willson (72) 4.) Kapahi (1979) 5.) Wills (1967)
6.) Kühr (1977) 7.) Cohen et al. (1977)

a) revised optical magnitude and classification, see notes on individual objects

b) new classification, see notes on individual objects

Table 5. Journal of the observations of S4 identifications

Object	date	telescope[a]	int.time [sec]	scale [Å/pixel]
(1)	(2)	(3)	(4)	(5)
0344+405	Nov 23, 1991	CA 2.2	3600	4.9
1152+551	June 27, 1992	CA 2.2	4000	5.2
1452+502	June 26, 1992	CA 2.2	4000	5.2
1745+624	July 1, 1992	CA 3.5	4000	4.3/3.6[b]
1833+653	July 2, 1992	CA 3.5	1000	4.3/3.6[b]
1849+670	July 3, 1992	CA 3.5	2000	4.3/3.6[b]
1926+611	July 28, 1990	CA 3.5	1800	4.3/3.6[b]
1943+546	June 27/28, 1992	CA 2.2	8000	5.2

a) CA 3.5 and CA 2.2 denote the 3.5m and the 2.2m telescopes on Calar Alto, Spain.

b) Twin spectrograph blue and red channel dispersion, respectively.

Table 6. Emission and absorption line data for S4 sources

Object	<z>	ID	λ_0 [Å]	λ_{obs} [Å]	z_{ind}	FWHM [Å]	EW_{obs} [Å]	Flux [10^{-16} erg/s/cm^2]	Remarks*
(1)	(2)	(3)	(4)	(5)	(6)	(7)	(8)	(9)	(10)
0344+405	0.039	MgI	5175	5379	0.039				gal
		NaI	5893	6126	0.040				gal
		NII	6584	6842	0.039	18.5	4.1	16.7:	cal
1152+551	0.050	CaII	3933	4125	0.049				gal
		CaII	3968	4158	0.048				gal
		G	4303	4516	0.050				gal
		MgI	5175	5439	0.051				gal
		NaI	5893	6193	0.051				gal
		Hα	6563	6918	0.054	15.4	4.6	32.8:	cal
1452+502	2.849	OVI	1034	3967	2.837	21.2	30.9	11.5	
		Lyα	1216	4680	2.849	26.8	312.9	73.0	
		CIV	1549	5970	2.854	43.8	141.8	34.9	
		HeII	1640	6323	2.855	21.4	12.6	2.7	
1745+624	3.886	OVI	1034	5048	3.882	82.6	83.6	35.6	
		Lyα	1216	5960	3.901	63.9	203.1	140.1	
		NV	1240	6061	3.888	104.4	113.4	76.4	
		OI	1306	6382	3.887	75.6	9.4	5.4	
		SiIV	1402	6832	3.873	79.8	22.6	12.3	atm
		CIV	1549	7553	3.876	64.9	64.7	32.9	atm
		MgII	2796	7886	1.820				abs
		MgII	2803	7914	1.823				abs
		MgII	2796	8584	2.070				abs
		MgII	2803	8626	2.077				abs
1833+653	0.161	G	4303	4991	0.160				gal
		MgI	5175	6008	0.161				gal
		NaI	5893	6848	0.162				gal
1849+670	0.657	MgII	2798	4639	0.658	56.9	23.2	42.9	
		OII	3727	6175	0.657	14.5	1.3	2.0	
		Hβ	4861	8058	0.658	169.6	102.5	107.6	
		OIII	4959	8207	0.655	37.1	11.5	13.9	
		OIII	5007	8290	0.656	26.8	20.9	27.2	
		MgII	2796	4287	0.533				abs
		MgII	2803	4299	0.534				abs
1943+546	0.263	CaII	3933	4971	0.264				gal
		CaII	3968	5010	0.263				gal
		MgI	5175	6530	0.262				gal
		NaI	5893	7430	0.261				gal
		Hα	6563	8296	0.264	27.9	15.1	2.9:	cal

*Abbreviations :
- abs : intervening absorption lines
- atm : emission line partially affected by the atmospheric B - or A - band
- cal : emission line flux uncertain due to uncorrected second order contamination of standard star spectra
- gal : stellar absorption lines of host galaxy

Table 7. Observed S5 radio sources

Object	other Name	RA (1950)	Dec (1950)	m	type	S_{5GHz}	α_{11-6}	FC
(1)	(2)	(3)	(4)	(5)	(6)	(7)	(8)	(9)
1027+744		10 27 13.38	+74 57 22.5	17.2	Gal	0.319	-0.20	1
1042+736	NGC 3343, UGC 5863 4C 73.10, 1072+73W1	10 42 23.66	+73 36 58.4	14.7	Gal	0.306	-0.63	1
1616+851		16 16 23.18	+85 09 26.1	17.4	Gal[a]	0.345	-0.60	0,1
1733+737		17 33 16.65	+73 42 09.1	18.0	Gal	0.277	-0.71	1
1807+707	4C 70.20	18 07 24.36	+70 44 13.5	17.5	Gal	0.476	-0.88	1
1945+726		19 45 55.33	+72 40 33.0	18.7	QSO	0.276	-0.81	1
1946+708		19 46 12.19	+70 48 22.6	18.0	Gal	0.636	-0.33	1
2111+801		21 11 07.60	+80 08 51.9	18.9	QSO	0.260	-0.37	1

References : 0.) this paper 1.) Kühr et al. (1987)

[a] revised classification, see notes on individual objects

Table 8. Journal of the observations of S5 identifications

Object	date	telescope[a]	int.time [sec]	scale [Å/pixel]
(1)	(2)	(3)	(4)	(5)
1027+744	July 2, 1992	CA 3.5	1800	4.3/3.6[b]
1042+736	July 1, 1992	CA 3.5	1000	4.3/3.6[b]
1616+851	June 27, 1992	CA 2.2	4000	5.2
1733+737	July 2, 1992	CA 3.5	2700	4.3/3.6[b]
1807+707	July 1, 1992	CA 3.5	1800	4.3/3.6[b]
1945+726	July 2, 1992	CA 3.5	2700	4.3/3.6[b]
1946+708	July 2, 1992	CA 3.5	2700	4.3/3.6[b]
2111+801	July 2, 1992	CA 3.5	900	4.3/3.6[b]

[a] CA 3.5 and CA 2.2 denote the 3.5m and the 2.2m telescopes on Calar Alto, Spain.

[b] Twin spectrograph blue and red channel dispersion, respectively.

Table 9. Emission and absorption line data for S5 sources

Object	<z>	ID	λ_0 [Å]	λ_{obs} [Å]	z_{ind}	FWHM [Å]	EW_{obs} [Å]	Flux [10^{-16} erg/s/cm^2]	Remarks*
(1)	(2)	(3)	(4)	(5)	(6)	(7)	(8)	(9)	(10)
1027+744	0.123	OII	3727	4187	0.123	6.9	4.3	3.9	
		NeIII	3869	4345	0.123	7.2	3.8	4.5	
		CaII	3933	4418	0.123				gal
		G	4303	4827	0.122				gal
		Hγ	4340	4869	0.122	14.7	3.7	7.4	
		OIII	4363	4893	0.121	22.5	7.6	15.5	
		Hβ	4861	5467	0.125	74.3	44.2	110.2	
		OIII	4959	5566	0.122	24.7	22.5	56.1	
		OIII	5007	5621	0.123	16.7	55.9	139.5	
		NaI	5893	6621	0.124				gal
		OI	6300	7079	0.124	13.0	1.4	4.5	
		Hα	6563	7366	0.122	81.9	55.3	177.8	
		Hα	6563	7370	0.123	20.9	23.1	74.5	
		NII	6584	7396	0.123	21.6	20.1	65.3	
		SII	6717	7546	0.123	6.1	1.6	5.0	
		SII	6731	7563	0.124	7.9	1.8	5.8	
1042+736	0.021	CaII	3933	4020	0.022				gal
		CaII	3968	4055	0.022				gal
		G	4303	4395	0.021				gal
		MgI	5175	5278	0.020				gal
		NaI	5893	6020	0.022				gal
1616+851	0.183	G	4303	5083	0.181				gal
		OIII	4959	5869	0.184	9.2	15.9	9.7	
		OIII	5007	5927	0.184	15.1	45.6	26.1	
		Hα	6563	7766	0.183	94.0	86.1:	26.4:	cal
1733+737	0.226	OII	3727	4569	0.226	14.6	14.5	5.9	
		CaII	3933	4823	0.226				gal
		CaII	3968	4865	0.226				gal
		G	4303	5272	0.225				gal
		MgI	5175	6353	0.228				gal
		NaI	5893	7235	0.228				gal
		Hα	6563	8040	0.225	32.9	3.9	7.2	
		NII	6584	8076	0.227	25.1	6.1	11.1	
1807+707	0.204	CaII	3933	4729	0.202				gal
		CaII	3968	4770	0.202				gal
		G	4303	5173	0.202				gal
		MgI	5175	6229	0.204				gal
		NaI	5893	7096	0.204				gal
		OIII	5007	6027	0.204	14.1	2.3	2.4	
		Hα	6563	7926	0.208	10.8	4.1	5.3	

Table 9. continued

Object	<z>	ID	λ_0 [Å]	λ_{obs} [Å]	z_{ind}	FWHM [Å]	EW_{obs} [Å]	Flux [10^{-16} erg/s/cm^2]	Remarks*
(1)	(2)	(3)	(4)	(5)	(6)	(7)	(8)	(9)	(10)
1945+725	0.303	OII	3727	4854	0.302	11.8	75.0	24.2	
		NeIII	3869	5036	0.302	10.5	21.7	7.4	
		NeIII	3968	5166	0.302	9.2	7.1	2.5	
		Hγ	4340	5659	0.304	14.0	10.4	4.5	
		OIII	4363	5689	0.304	7.6	4.3	1.9	
		HeII	4686	6110	0.304	7.2	2.7	1.4	
		Hβ	4861	6340	0.304	10.8	15.9	9.8	
		OIII	4959	6468	0.304	9.5	55.8	32.8	
		OIII	5007	6531	0.304	11.7	202.6	113.3	
		NI	5199	6782	0.304	9.3	3.1	1.6	
		OI	6300	8211	0.303	20.3	21.2	12.4	
		Hα	6563	8544	0.302	101.7	146.9	161.3	
		Hα	6563	8551	0.303	8.6	25.8	28.3	
		NII	6584	8576	0.303	18.4	32.2	34.7	
		SII	6717	8747	0.302	15.1	12.6	11.9	
		SII	6731	8766	0.302	23.9	20.6	18.4	
1946+708	0.101	OII	3727	4104	0.101	9.4	41.4	3.7	
		G	4303	4734	0.100				gal
		MgI	5175	5697	0.101				gal
		NaI	5893	6488	0.101				gal
		OI	6300	6938	0.101	11.4	3.9	6.5	
		Hα	6563	7227	0.101	11.2	17.1	28.4	
		NII	6584	7248	0.101	24.7	12.7	20.9	
		SII	6717	7396	0.102	10.6	6.1	9.9	
		SII	6731	7414	0.101	18.9	9.5	15.5	
2111+801	0.524	MgII	2798	4267	0.525	82.9	186.2	24.2	
		OII	3727	5680	0.524	10.3	23.2	4.9	
		NeIII	3869	5896	0.524	11.7	18.5	4.1	
		NeIII	3968	6048	0.524	12.9	11.9	2.2	
		Hγ	4340	6616	0.524	23.4	19.8	3.9	
		OIII	4363	6651	0.524	25.0	29.1	5.9	
		Hβ	4861	7410	0.524	14.3	27.7	5.7	
		Hβ	4861	7435	0.530	134.4	92.3	19.2	
		OIII	4959	7558	0.524	13.8	62.8	15.0	
		OIII	5007	7631	0.524	14.5	114.9:	22.6:	atm

*Abbreviations :
- atm : emission line partially affected by the atmospheric B - or A - band
- cal : equivalent width and emission line flux uncertain due to uncorrected second order contamination of standard stars
- gal : stellar absorption lines of host galaxy

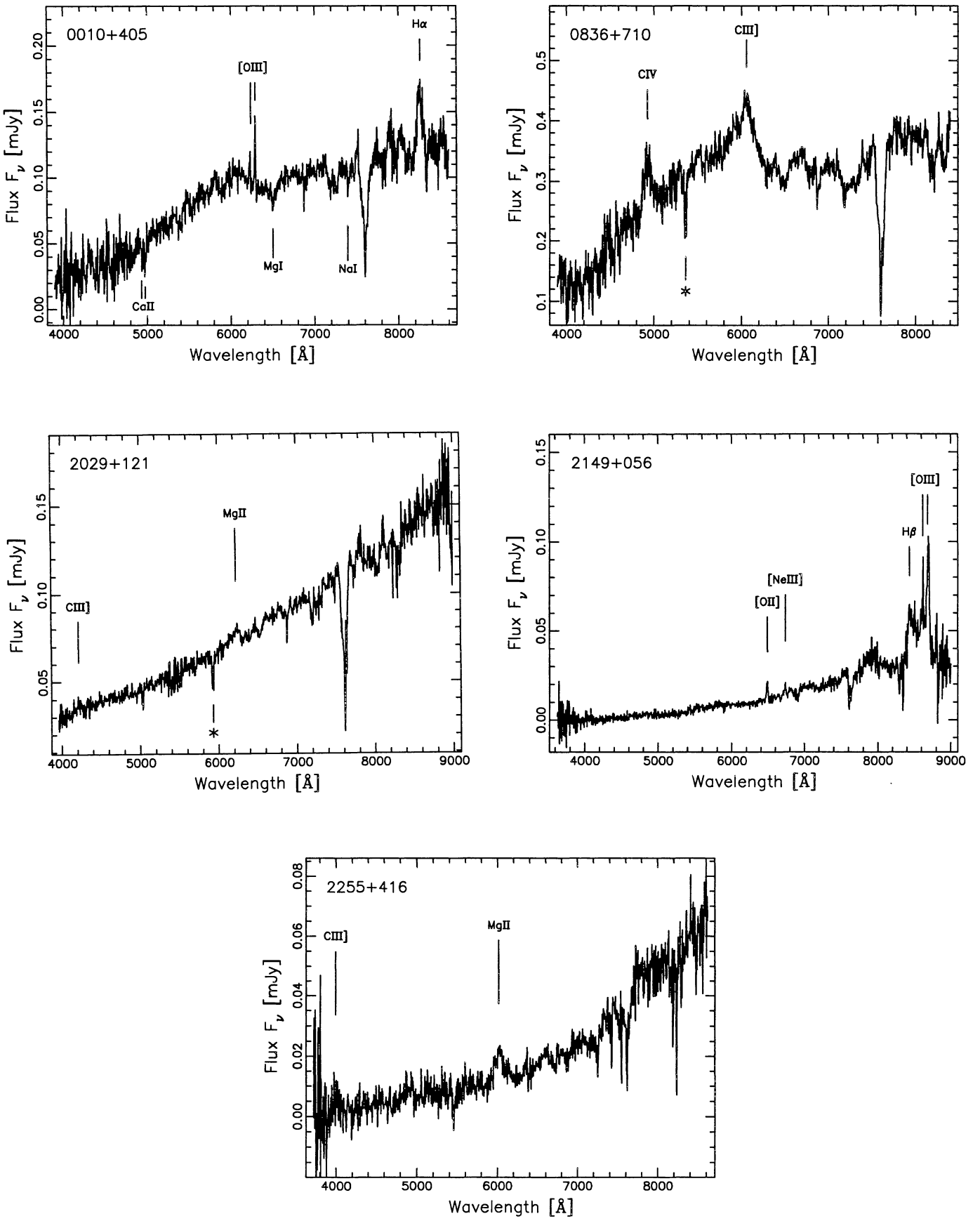

Fig. 1. Optical spectra of 1 Jy radio source identifications. Identified spectral features are marked

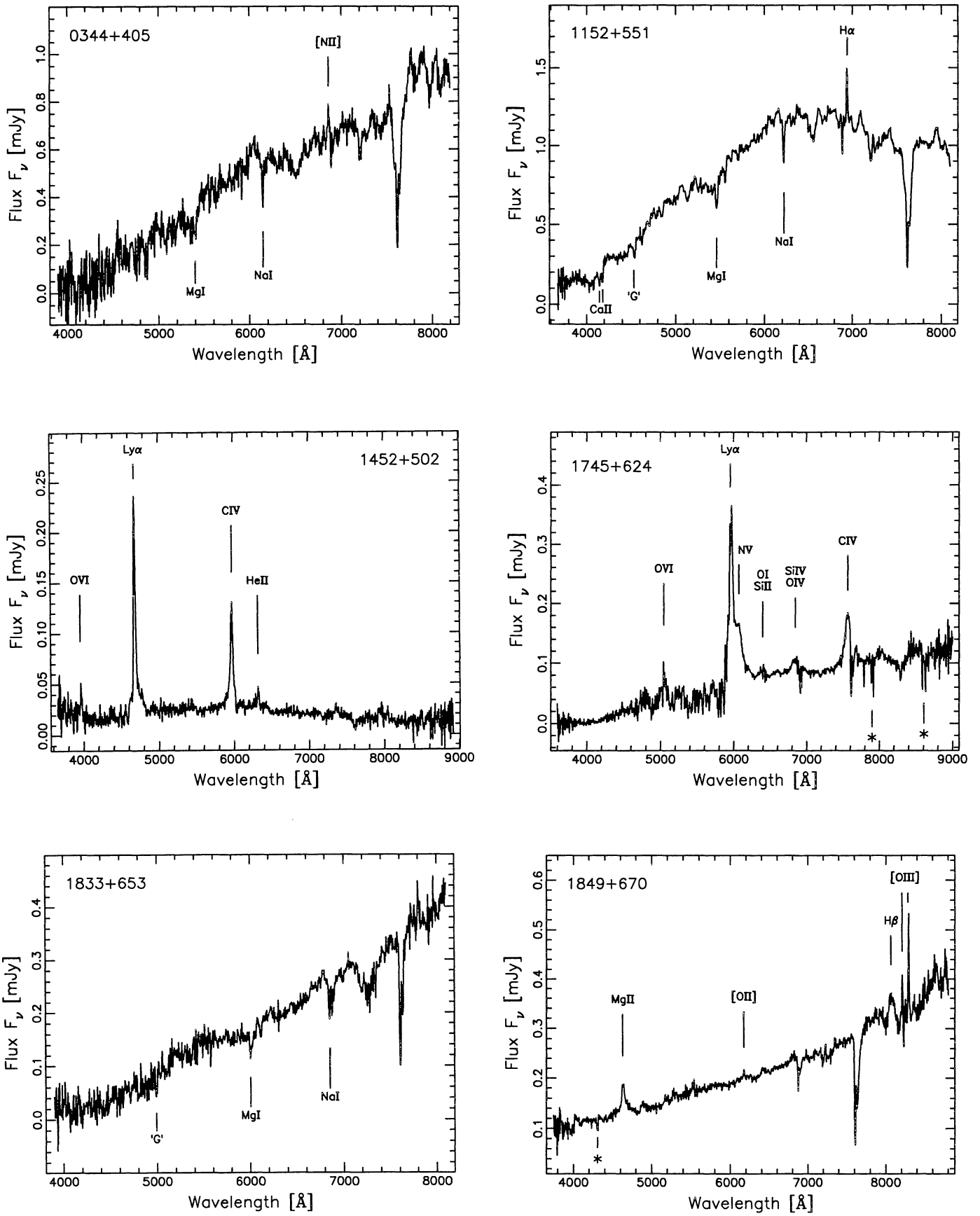

Fig. 2. Optical spectra of S4 radio source identifications. Identified spectral features are marked

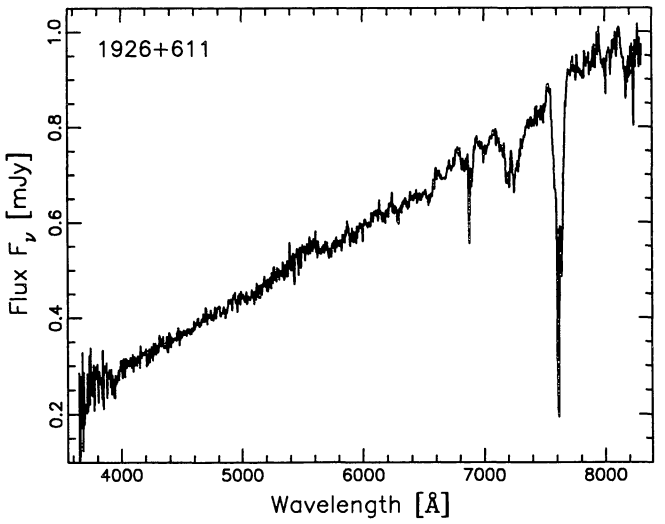

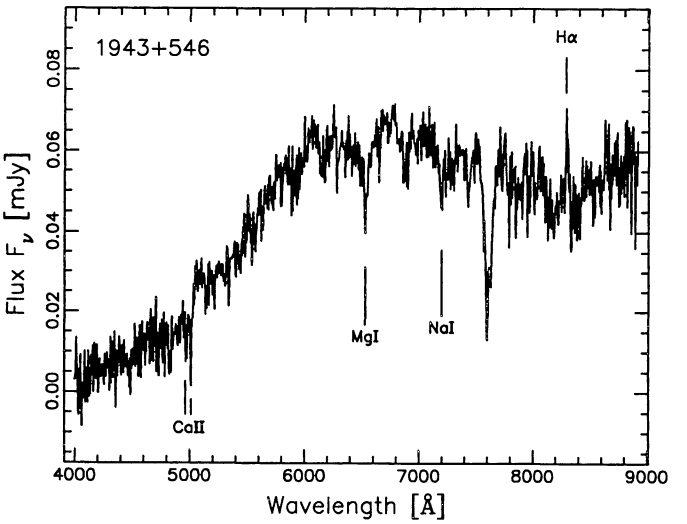

Fig. 2. continued

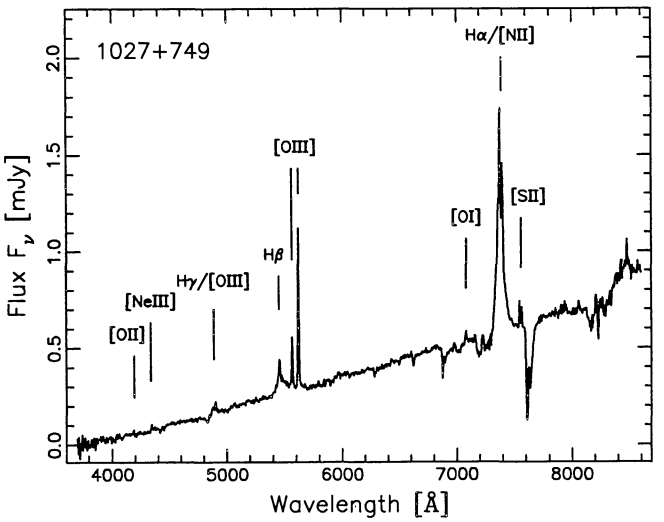

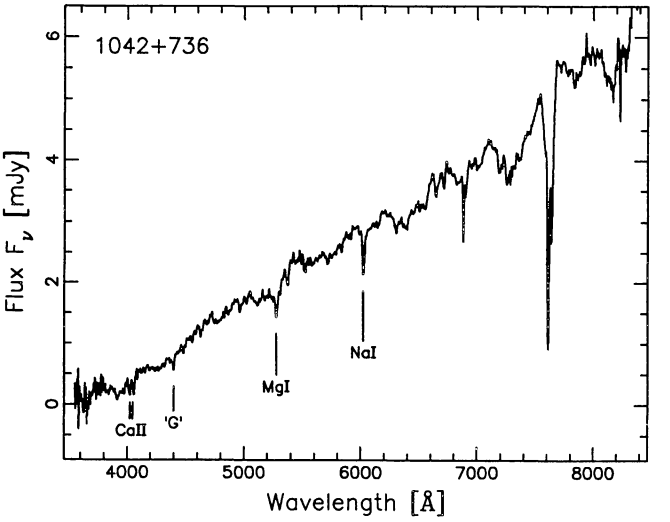

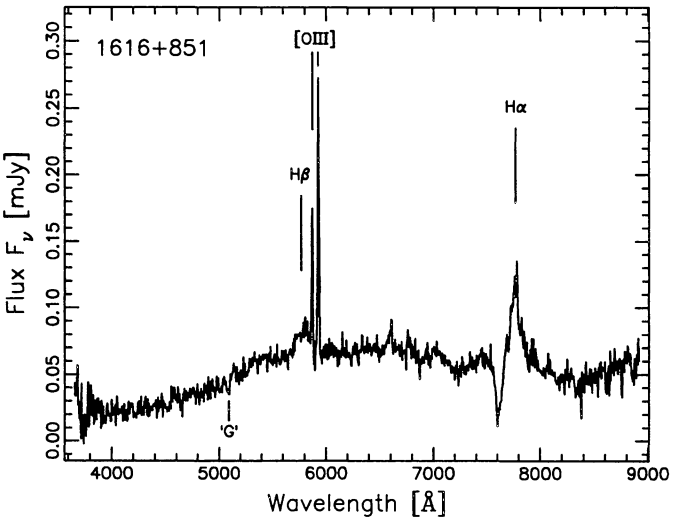

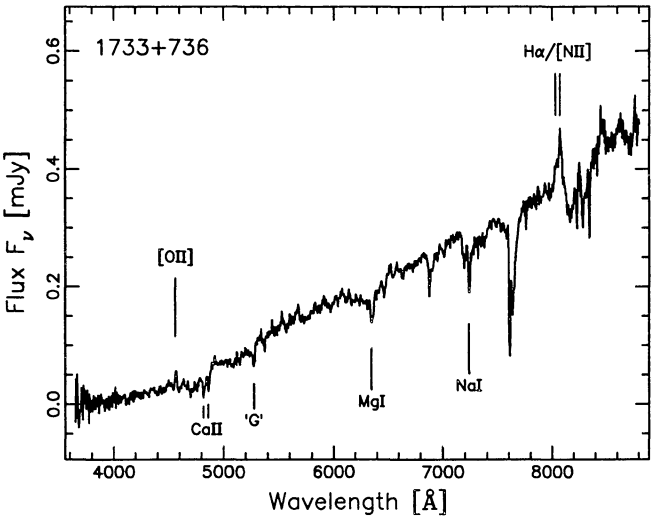

Fig. 3. Optical spectra of S5 radio source identifications. Identified spectral features are marked

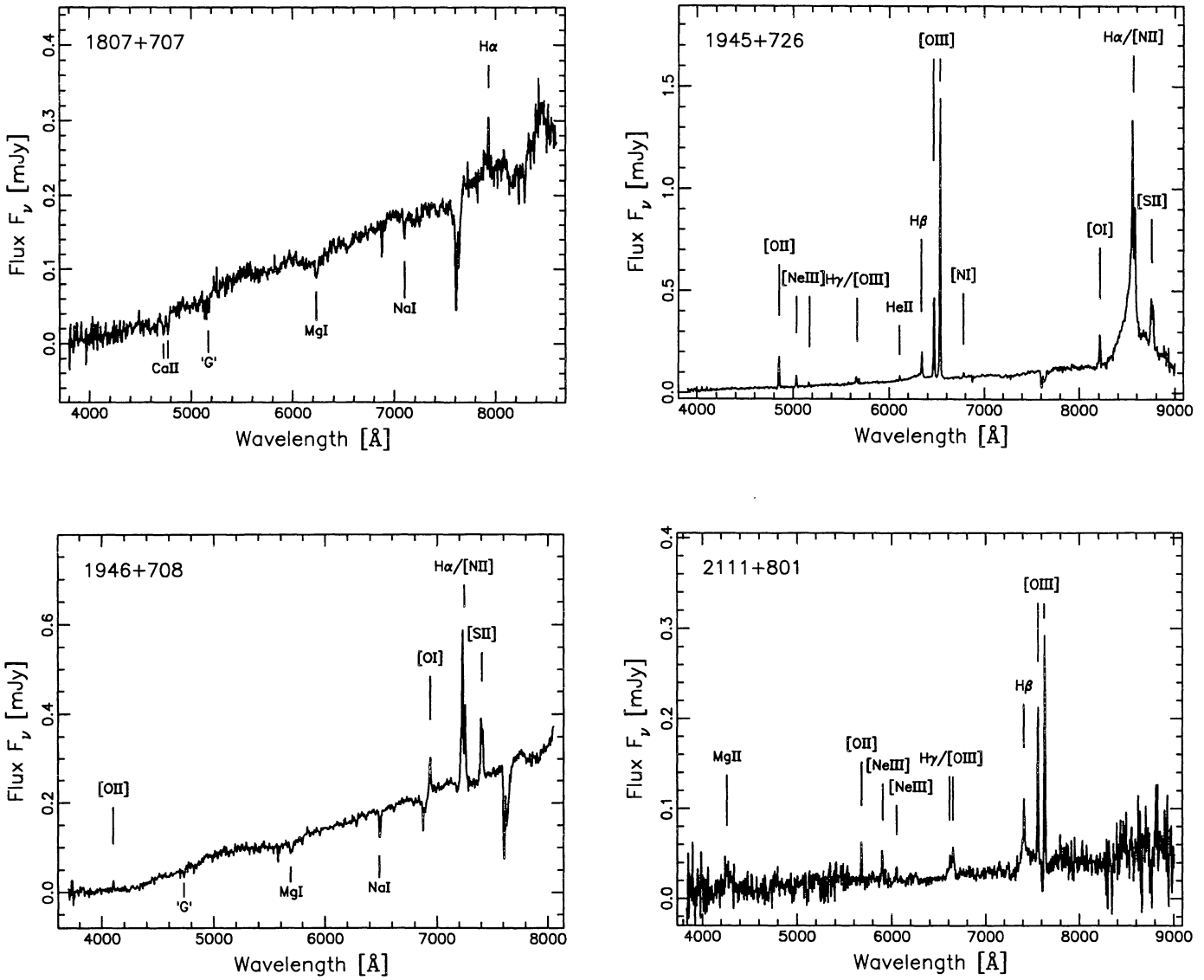

Fig. 3. continued

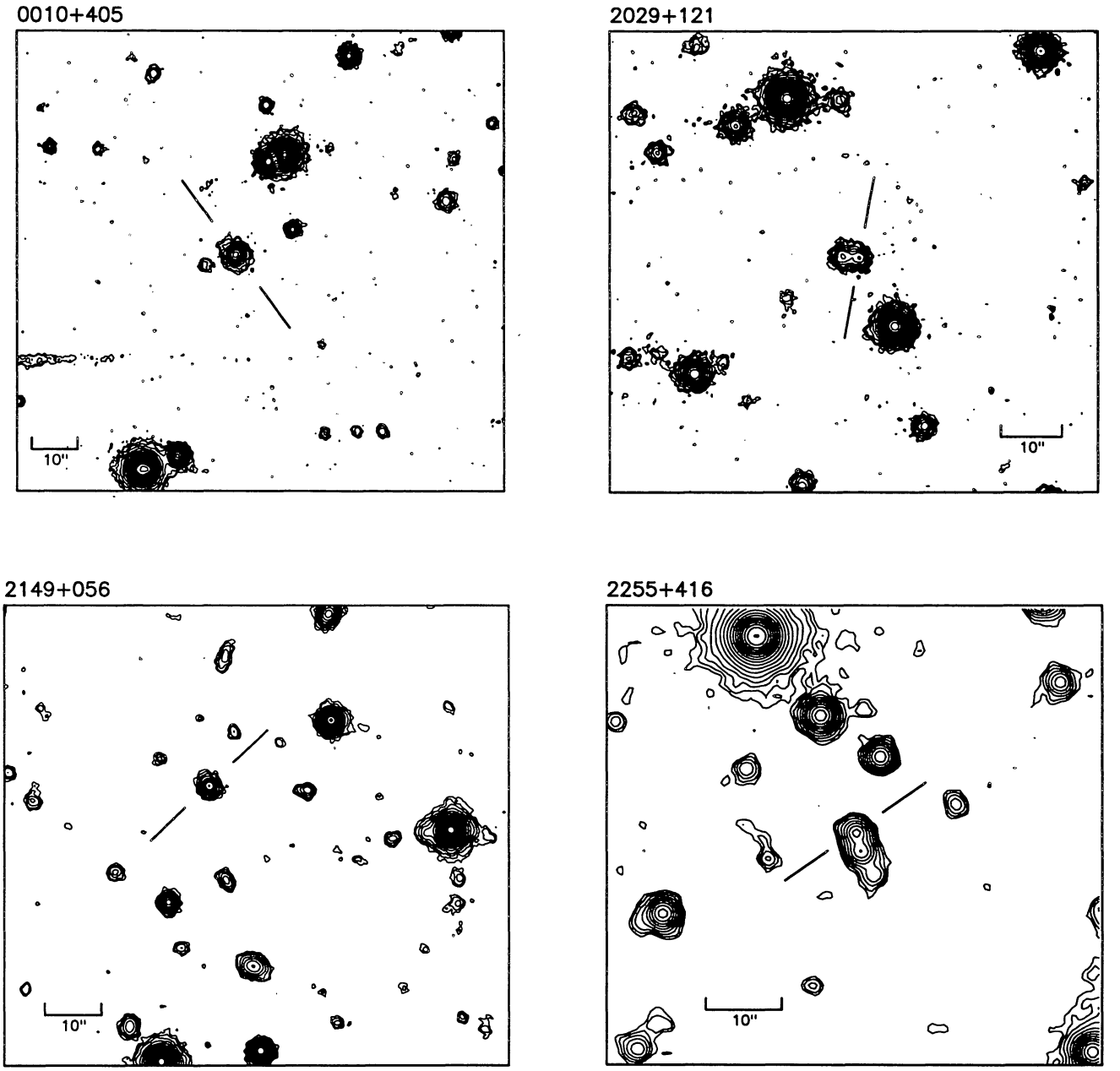

Fig. 4. R – band CCD images of the 1 Jy sources 0010+405, 2029+121, 2149+056 and 2255+416. North is up and east to the left. The identifications of the radio sources are marked.

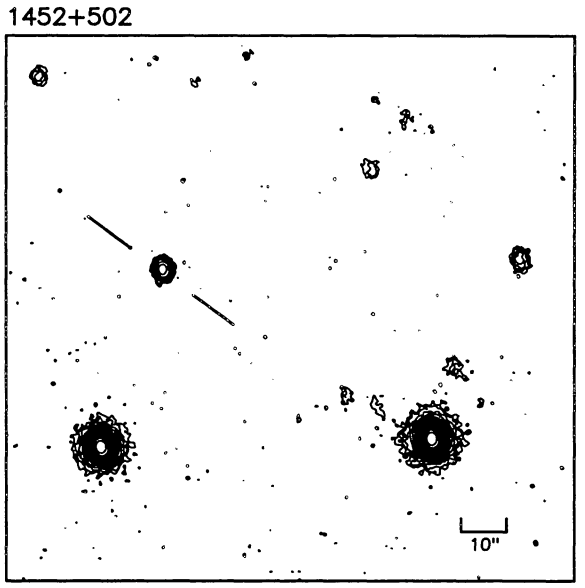

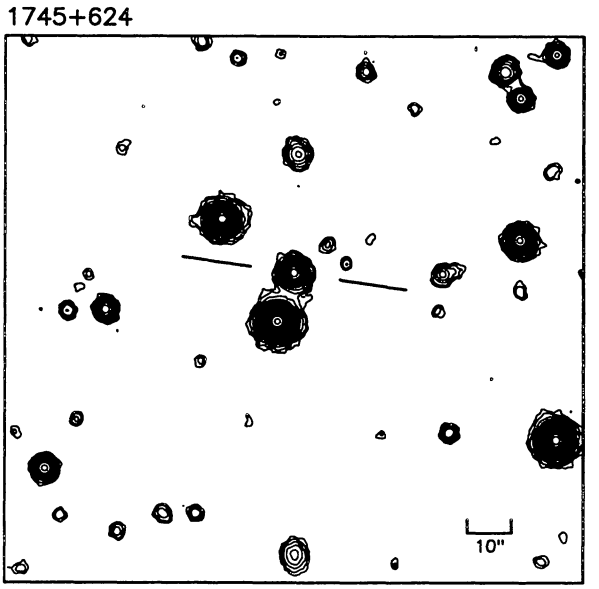

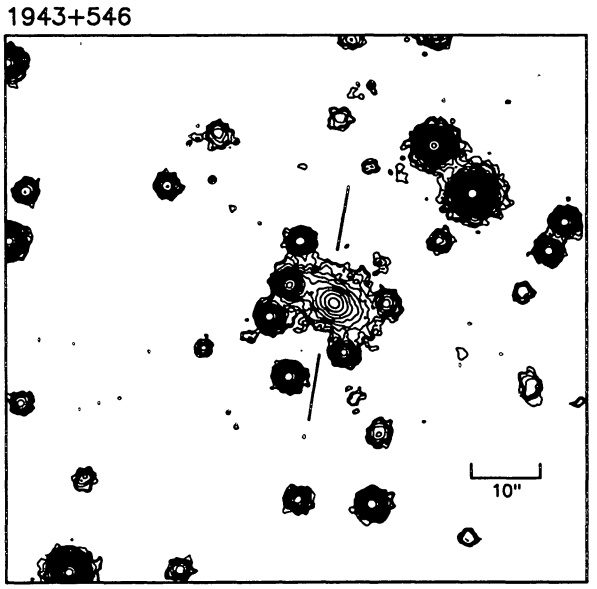

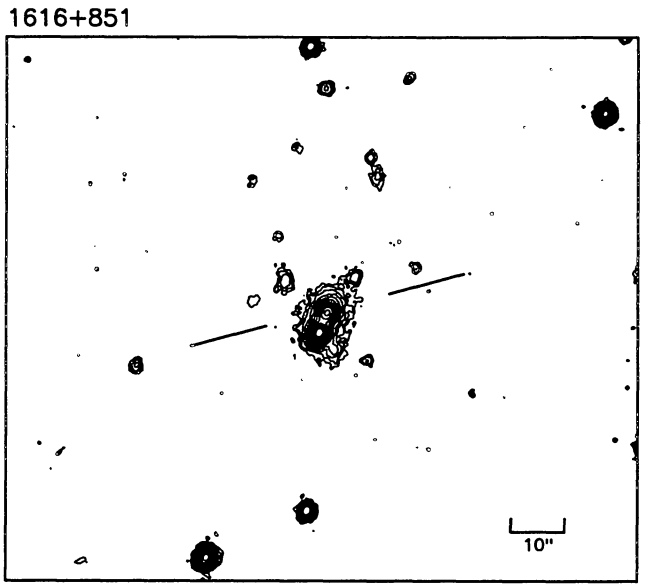

Fig. 5. Direct R – band images of the S4 sources 1452+502, 1745+624 and 1943+546. North is up and east to the left. The identifications of the radio sources are marked

Fig. 6. Direct R – band images of the S5 sources 1616+851. North is up and east to the left. The identification of the radio source is marked